micromachines

Article

Effect of β-PVDF Piezoelectric Transducers' Positioning on the Acoustic Streaming Flows

Susana O. Catarino [1,2,*], **João Mário Miranda** [1] **and Graça Minas** [2]

[1] Transport Phenomena Research Center, Department of Chemical Engineering, Faculty of Engineering, University of Porto, 4200-465 Porto, Portugal; E-Mail: jmiranda@fe.up.pt

[2] Centro Algoritmi, University of Minho, Campus de Azurém, 4800-058 Guimarães, Portugal; E-Mail: gminas@dei.uminho.pt

* Author to whom correspondence should be addressed; E-Mail: scatarino@dei.uminho.pt; Tel.: +351-253-510-190.

Abstract: This paper reports the numerical and experimental analysis of the acoustic streaming effect in a fluidic domain. The actuation of a piezoelectric transducer generates acoustic waves that propagate to the fluids, generating pressure gradients that induce the flow. The number and positioning of the transducers affect the pressure gradients and, consequently, the resultant flow profile. Two actuation conditions were considered: (1) acoustic streaming generated by a 28 μm thick β-poly(vinylidene fluoride) (β-PVDF) piezoelectric transducer placed asymmetrically relative to the fluidic domain and (2) acoustic streaming generated by two 28 μm thick β-PVDF piezoelectric transducers placed perpendicularly to each other. The transducers were fixed to the lower left corner of a poly(methyl methacrylate) (PMMA)cuvette and were actuated with a 24 Vpp and 34.2 MHz sinusoidal voltage. The results show that the number of transducers and their positioning affects the shape and number of recirculation areas in the acoustic streaming flows. The obtained global flows show great potential for mixing and pumping, being an alternative to the previous geometries studied by the authors, namely, a single transducer placed symmetrically under a fluidic domain.

1. Introduction

One of the major requirements for a fully-integrated microfluidic device is the ability to automatically mix and control fluids in a reasonable time [1,2]. However, in microfluidic systems, the Reynolds number is usually less than 1 and, consequently, molecular diffusion becomes the main mixing mechanism, which leads to overall slow processes.

In recent years, acoustic streaming has become one of the most effective techniques, with no mechanical parts, for promoting mixing and pumping in fluidic devices [2–5], since this technique overcomes the limitations of mixing in micro scale systems. Many authors have approached this phenomenon of acoustic streaming through numerical simulations and experimental studies [4,6–10]. Typically, acoustic streaming uses a piezoelectric transducer for generating acoustic waves that are absorbed by the fluids. This mechanism promotes pressure gradients that, when properly induced, generate the fluid flow and mixing [11–13]. Specifically, the harmonic oscillation of the solid boundary near the fluid generates the propagation of the acoustic waves in the fluid as well as a steady mean flow field [12].

In particular, one of the materials that has received much attention due to its piezoelectric properties and advantages relatively to the most traditional piezoelectric material (such as the ceramics or quartz) is the poly(vinylidene fluoride) (PVDF) polymer in its β phase [14–16]. This material has one of the best piezoelectric responses among polymers (as examples of d_{33} values of several polymers, 35 pC/N for PVDF, 33.5 pC/N for P(VDF-TrFE), 2 pC/N for Parylene-C or 16.5 pC/N for PI (β-CN) APB/ODPA [17,18]) and has great potential for microprocessing and integration in microdevices, since it can be easily deposited into thin-films. PVDF, when processed in the β phase, presents good mechanical, acoustic and thermal properties. Specifically, PVDF presents low acoustic and mechanical impedances, which are important characteristics for the generation and propagation of acoustic waves in fluids. PVDF is transparent (higher than 70% in the visible spectral range [19]), which is also an important requirement for lab-on-a-chip devices comprising optical detection, mainly when the transducer is located in the optical path [16].
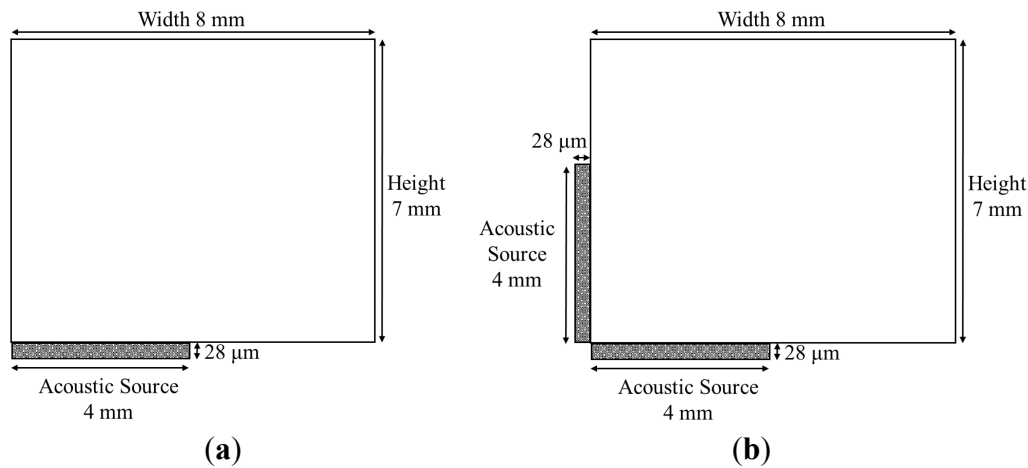
Relative to the acoustic streaming numerical studies, the most relevant works in the field are focused on the acoustic propagation and streaming between parallel plates with infinite extent, as approached by Nyborg [13] or within cylindrical channels of constant cross-section and infinite length, as approached by Frampton [4]. Additionally, the majority of the studies (following the early research of Eckart [20] and Nyborg [13]) consider SAW devices [21,22] or plane travelling waves, while the present work is focused in non-planar waves, generated by a transducer with a small width when compared with the cuvette width. Since most of the acoustic mixing studies are based on ceramic piezoelectric transducers (examples in [23,24]), this work brings a new perception of the use of piezoelectric polymeric thin-films as acoustic transducers, actuated at high frequencies.

From previous work, it is already known how the acoustic propagation occurs when the fluid domain is actuated at 10 MHz by a single piezoelectric transducer centered relatively to the fluidic domain [25,26]. Therefore, the present work is focused on studying the acoustic streaming propagation and consequent global flows in a 2D domain (which is representative of a 3D domain) actuated by a transducer placed asymmetrically relatively to the fluidic domain (Figure 1a), and by two perpendicular transducers (as represented in Figure 1b) in order to evaluate the potential of this

positioning for pumping applications and compare it with the previous geometries with a single centered transducer [26]. Through this analysis, we will evaluate the effect of the acoustic waves superposition and of the acoustic reflections in the global flows profiles.

By adding numerical simulations of the same arrangement as the one presented in Figure 1, but at microscale (0.8 mm × 0.7 mm cuvette and 0.4 mm length transducers), this paper also intends to study the potential of the simultaneous actuation of two transducers for implementation in microdevices.

Figure 1. Macroscale version of the cuvette and piezoelectric transducers positioning for studying the acoustic streaming phenomena. (**a**) One transducer. (**b**) Two transducers perpendicularly placed.

Mathematical Model

The numerical model of the acoustic streaming phenomenon generated by a piezoelectric transducer consists of a multiphysics problem comprising the piezoelectric effect, the piezo-fluid interface, the acoustic propagation and the global steady streaming. Each one of these mechanisms can be mathematically described by a proper set of equations.

The piezoelectric effect comprises the differential Equations (1) and (2), two constitutive equations of the piezoelectric material (3) and (4) and the Hooke's law (5) [3].

$$\rho \frac{d^2 \mathbf{m}}{dt^2} - \nabla \cdot \mathbf{M} = \mathbf{b} \tag{1}$$

$$\nabla \cdot \mathbf{D} = 0 \tag{2}$$

$$\mathbf{S} = \mathbf{s}^{\mathbf{E}} \mathbf{M} + \mathbf{d}^{\mathbf{M}} \mathbf{E} \tag{3}$$

$$\mathbf{D} = \boldsymbol{\varepsilon}^{\mathbf{M}} \mathbf{E} + \mathbf{d}^{\mathbf{E}} \mathbf{M} \tag{4}$$

$$\mathbf{S} = (\nabla \mathbf{m} + (\nabla \mathbf{m})^{\mathrm{T}}) / 2 \tag{5}$$

In the above equations, ρ is the density, $\mathbf{M}$ the mechanical stress, $\mathbf{m}$ the mechanical displacement of the piezoelectric material, $\mathbf{b}$ the volume force vector actuating in the piezoelectric material, $\mathbf{D}$ the electrical displacement, $\mathbf{d}^{\mathbf{M}}$ and $\mathbf{d}^{\mathbf{E}}$ the piezoelectric coefficients, $\mathbf{E}$ the electric field, $\mathbf{S}$ the mechanical strain, $\boldsymbol{\varepsilon}^{\mathbf{M}}$ the dielectric permittivity and $\mathbf{s}^{\mathbf{E}}$ the elastic coefficient. The β-PVDF parameters are listed

in [17]. Relatively to the electric boundary conditions, the transducer boundary in contact with the cuvette is connected to the ground, the opposite boundary is connected to a sinusoidal voltage (with fixed amplitude and frequency) and the lateral faces of the transducer present electric continuity.

The piezoelectric effect generates acoustic waves that propagate into the fluid. As predicted from the piezoelectric constitutive equations, the amplitude of the pressure waves in the transducer-fluid interface is directly proportional to the transducer electric voltage actuation. In the present work, the maximum voltage limit was established by the 24 Vpp DC source and, therefore, 24 Vpp was selected as the actuation voltage, both in numerical and experimental tests. The propagation of these waves to the fluids depends on the interface pressure, frequency and fluid properties (density, viscosity and speed of sound), as well as the acoustic matching layers (that can absorb or reflect the acoustic waves). Therefore, the numerical simulations of the acoustic streaming flows are based on the compressible Navier-Stokes momentum (6) and continuity (7) equations, where ρ is the fluid density, $\mathbf{u}$ the velocity field vector, p the pressure, η the dynamic viscosity, κ the dilatational viscosity, $\mathbf{F}$ the volume force field and $\mathbf{I}$ the identity matrix.

$$\rho \frac{d\mathbf{u}}{dt} + \rho\,\mathbf{u}\cdot\nabla\mathbf{u} = \nabla\cdot\left[-p\mathbf{I} + \eta(\nabla\mathbf{u} + (\nabla\mathbf{u})^{\mathrm{T}}) - (\frac{2\eta}{3} - \kappa)(\nabla\cdot\mathbf{u})\mathbf{I} \right] + \mathbf{F} \tag{6}$$

$$\frac{d\rho}{dt} + \nabla\cdot(\rho\,\mathbf{u}) = 0 \tag{7}$$

The acoustic streaming boundary conditions are detailed in [25]. The piezo-fluid boundary is defined by a vector with normal and tangential components, correspondent to the stress generated by the piezoelectric transducer, stating that the stress is a continuous function across the boundary.

The acoustic streaming problem must be decomposed in two subproblems, one directed to short timescales and another to long timescales, in order to overcome the large difference between the piezoelectric vibration and fluid flow timescales [27]. This procedure is based on the Nyborg approach [13], firstly developed in 1953, that considers an acoustic driving force, obtained from the instantaneous propagation of the acoustic waves, which affects the global acoustic flow. This approach was followed by several authors [3,4,9,11,28], who developed significant studies in the numerical acoustic streaming simulation at microscale, based on the instantaneous acoustic propagation time averaging. In this procedure, the Navier-Stokes variables (pressure, density and velocity) are expanded in zero order, first order and second order components. The first order variables represent the instantaneous acoustic flow, as these variables describe the damped propagation of the acoustic wave. After solving the first order equations, a time averaged acoustic force is determined. The time averaged value is obtained by integration of the Navier-Stokes force term during one wave period (after the periodic solution stabilization) followed by its division by the wave period. The time averaged force is then applied as the source term for solving the second order Navier-Stokes equations. This second order problem describes the steady global flow, that represents the average acoustic streaming effects in a large time scale [4,9,25].

The mathematical model was solved for the cuvettes represented in Figure 1, in order to evaluate the acoustic streaming generated by β-PVDF transducers. The numerical model was implemented in a commercial software (COMSOL Multiphysics, Burlington, MA, USA). The first order equations were solved in a transient simulation during 50 μs, with a 1 ns time step, while the second order equations

were solved in a stationary state. The first and second order problems were solved using an unsymmetric multifrontal sparse LU factorization package solver, with 1×10^{-8} relative tolerance and 10,000 maximum number of iterations. The domain was meshed with a structured quadrilateral mesh, where each element has a 1.67 μm × 3.33 μm dimension, which guarantees about 26 elements for each acoustic wavelength in the propagation distance. The effect of the mesh dimensions in the acoustic streaming results is discussed in [25]. In addition to the numerical simulations, some experimental tests were performed with a prototype system, for validating the simulated flows and evaluating the performance of β-PVDF thin-films for acoustic transducers applications.

## 2. Experimental Setup and Transducer Electrical Characterization

In the acoustic streaming experimental tests, the authors used 28 μm thick β-PVDF transducers to generate the acoustic waves. β-PVDF transducers were fabricated through spin-coating techniques [19]. Iniatially, in order to electrically characterize the β-PVDF transducers, we developed a prototype with eight transducers, each with a 2 × 2 cm^2 area. The prototype consisted of a Printed Circuit Board (PCB) with the corresponding Radio Frequency (RF) connectors, with the 28 μm thickness β-PVDF transducers glued to it, as shown in Figure 2. The transducers were glued to the PCB with silver conductive paint, since this material fixes the transducer without blocking the piezoelectric vibration. The mechanical damping of the silver conductive paint was neglected in the simulations.

Figure 2. Printed Circuit Board with Radio Frequency (RF) connectors and the 2 × 2 cm^2 β-poly(vinylidene fluoride) (β-PVDF) (28 μm thickness) transducers, with aluminum electrodes, glued to the Printed Circuit Board (PCB).

After fabrication of the prototype, the β-PVDF transducers were electrically characterized using a previously calibrated Vector Network Analyzer (VNA) F8357A from Agilent. The VNA experimental curve, presented in Figure 3, was obtained after connecting the RF connectors of the prototype to the VNA (without electric matching circuit) and measuring the *S*-parameters for a frequency range up to 100 MHz. The *S*-parameters are determined from the amplitude and phase of the reflected and transmitted waves and describe the electric energy reflection in the transducer input. These *S*-parameters correspond to the elements of a dispersion matrix, and each specific element of the matrix is given by $S_{ij} = V_i^- / V_j^+$, where V_j^+ is the amplitude of the incident voltage wave and V_i^- is the amplitude of the emergent (reflected) wave. In particular, the S_{11} parameter corresponds to the non-dimensional reflection coefficient and allows us to quantify the electric signal amplitude that effectively actuates the transducer [29].

Figure 3. Vector Network Analyzer (VNA) curve of the S_{11} parameter (reflection coefficient) measured for the 28 μm thickness PVDF transducer without electric matching.
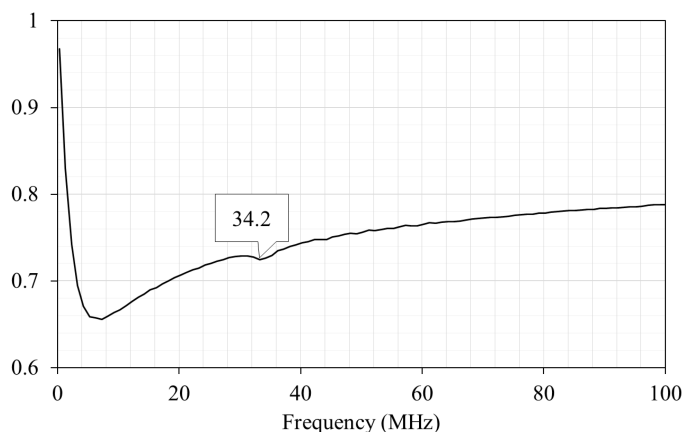

In order to optimize the acoustic transmission, the actuation frequency must equal the mechanical resonance frequency of the transducer, which is given by $Fr = c/2t$, where Fr is the resonance frequency, c the speed of the sound and t the thickness of the transducer. Since the β-PVDF films have a 28 μm thickness and the speed of sound in PVDF is 2.2 km/s, the theoretical resonance frequency is 39 MHz. Therefore, the transducer must show smaller reflection coefficient values around the theoretical resonance frequency, indicating maximum transmission. A small oscillation (indicative of minor electric reflected signal) was detected in the VNA curve at 34.2 MHz (Figure 3) and, consequently, a matching circuit for electric driving at this frequency was implemented, for enhancing the electrical transmission for the transducers and improve the vibration, limiting the electric transmission in all the other frequencies. The resonance frequency deviation, relatively to the expected 39 MHz, results from the experimental setup interferences (copper wire, silver conductive paint and RF connectors) that are not removed by the system calibration. Figure 4 shows the schematic of the 34.2 MHz matching circuit and the VNA curve of the piezoelectric transducer after implementation of the matching circuit. The matching circuit was designed based on the Smith diagram [29] obtained through the VNA measurements, and optimized in the Ansoft Designer software. The Smith diagram consists of a polar representation of the reflection coefficient and is an auxiliary tool in the electric matching process, which occurs by adding impedance and/or admittance components, in series or parallel [29]. The quality of the matching circuit for improving the electric transmission at 34.2 MHz was experimentally evaluated through a VNA analysis, presented in Figure 4b.

After the electrical characterization of the transducers, they were actuated by a 9 dB RF signal, using a RF Signal Generator (N9319A from Agilent, Santa Clara, CA, USA) for generating a sinusoidal signal with constant frequency and a RF amplifier (Coaxial Amplifier ZHL-6A from Mini-Circuits, Brooklyn, NY, USA) to guarantee enough power to actuate the transducers, connected to a 24 Vpp DC source.

Poly(methyl methacrylate) (PMMA) cuvettes (Figure 5) with 8 mm width, 7 mm height and 2.5 mm thickness were fabricated and used to determine the streaming patterns in the cuvettes. The slight curve over the cuvette thickness, observed in Figure 5, was neglected in the two dimensional numerical simulations.

Figure 4. (**a**) Scheme of the electric matching circuit for the PVDF actuation. (**b**) VNA curve of the S_{11} parameter (reflection coefficient) measured for the 28 μm thickness PVDF transducer after electric matching implementation. The minimum reflection peak is located at 34.2 MHz.

(**a**) (**b**)
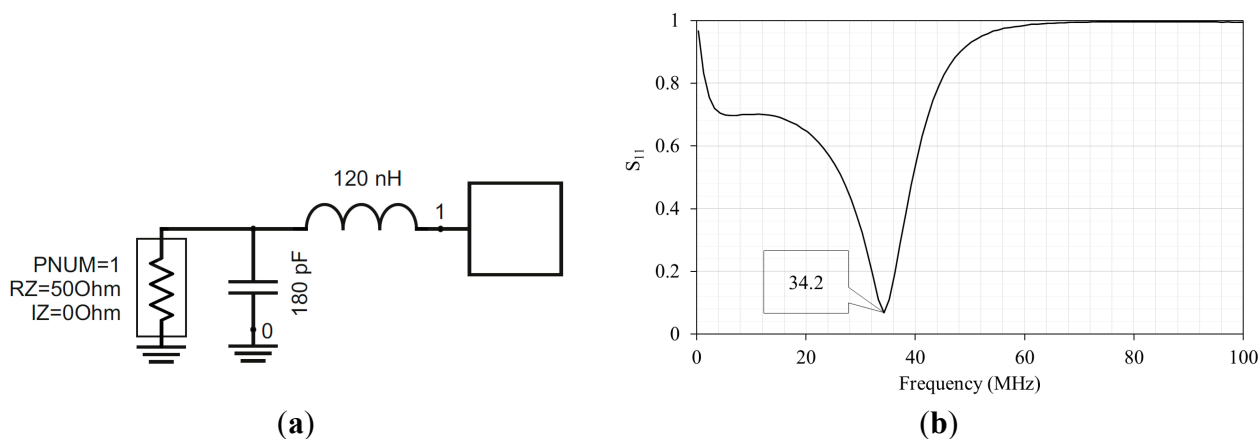
Figure 5. Poly(methyl methacrylate) (PMMA) cuvette, with 8 mm width, 7 mm height and 2.5 mm thickness used in the acoustic streaming experimental tests.
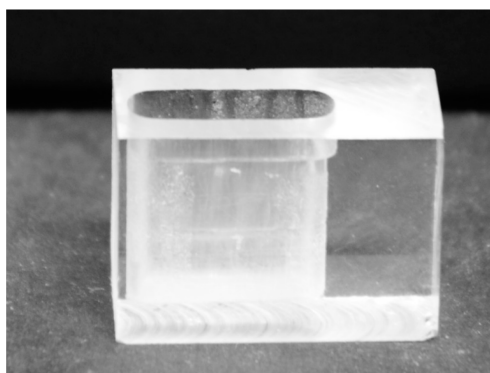
The streaming patterns were assessed by a simplified PIV (Particle Image Velocimetry) white light system, using 10 μm diameter polystyrene particles suspended in water. Image processing tools ImageJ and PIVlab [30] were used for processing the PIV results, in order to determine the streaming patterns. Each PIV measurement was performed during one minute with a HDR-UX7E camera from Sony (Tokyo, Japan), with 6.1 megapixel spatial resolution and using a 10 fps sampling rate. Since the cuvette walls have a low thickness (1 mm) the acquisition system was able to capture the particles flow in the cuvette.

The experimental results were compared to numerical results, obtained by solving the piezoelectric and first and second order Navier-Stokes equations (the detailed model can be found in [25]). The same actuation and experimental conditions were considered, as were the water properties at room temperature.

3. Results and Discussion

Over the last years, the authors have studied a single transducer placed centrally in the bottom of the cuvette, through numerical simulations and experimental tests [25,31]. The obtained results agreed with the results expected from the literature [7,9]. Therefore, in this paper, the authors solved the

previously validated model for two different transducers arrangements, in order to draw conclusions about the effect of the transducer placement in the acoustic streaming flows.

3.1. Acoustic Streaming Patterns in the Cuvette

The acoustic streaming patterns were evaluated in an 8 mm width × 7 mm height cuvette (Figure 1). Numerically, the global flow was obtained after simulation of the first and second order Navier-Stokes equations (as referred in Section 1.1), considering the properties of water at room temperature. Experimentally, after recording the movies of the particle movements, the authors extracted equally time distributed frames. Those frames were analyzed in imageJ software, where they were processed (subtraction of the background and use of thresholds) in order to obtain black and white images containing the particles. Finally, the obtained images were imported by PIVlab software and the average flow vectors were calculated.

Figure 6 presents the simulated streamlines and flow vectors, for better comparison with the experimental results, and the experimental acoustic streaming vectors, in the 8 mm width × 7 mm height cuvette with a 4 mm length piezoelectric transducer, placed asymmetrically in the bottom of the cuvette (Figure 1a).

Figure 6. (**a**) Velocity magnitude (m/s) with streamlines (**left**) and flow vectors (**right**), in the 8 mm width × 7 mm height cuvette with one 4 mm length transducer, considering a 24 Vpp and 34.2 MHz oscillatory excitation, after a stationary simulation of the second order Navier-Stokes equations. (**b**) Experimental flow vectors obtained in PIVlab.
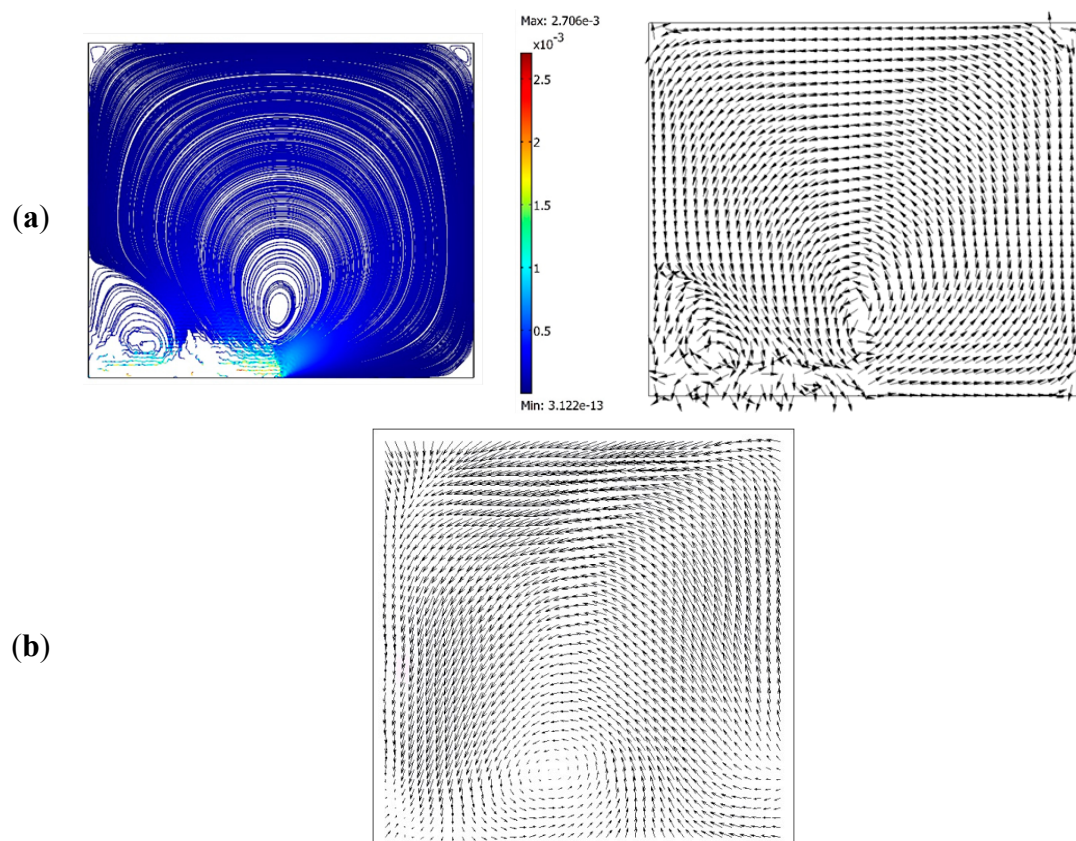
Figure 6 shows the formation of a large recirculation area when a single transducer is asymmetrically placed under the cuvette, complemented by a small vortex in the lower left corner of the fluidic domain, near the transducer, as a result of the acoustic attenuation in the domain. The experimental global flow agrees with the numerical results.

Figure 7 presents the simulated streamlines and flow vectors, for better comparison with the experimental results, and the experimental acoustic streaming vectors, in the 8 mm width × 7 mm height cuvette with two 4 mm length transducers, perpendicularly placed in the lower left corner of the cuvette (Figure 1b).

Figure 7. (**a**) Velocity magnitude (m/s) with streamlines (**left**) and flow vectors (**right**), in the 8 mm width × 7 mm height cuvette with two 4 mm length transducers, considering a 24 Vpp and 34.2 MHz oscillatory excitation, after a stationary simulation of the second order Navier-Stokes equations. (**b**) Experimental flow vectors obtained in PIVlab.
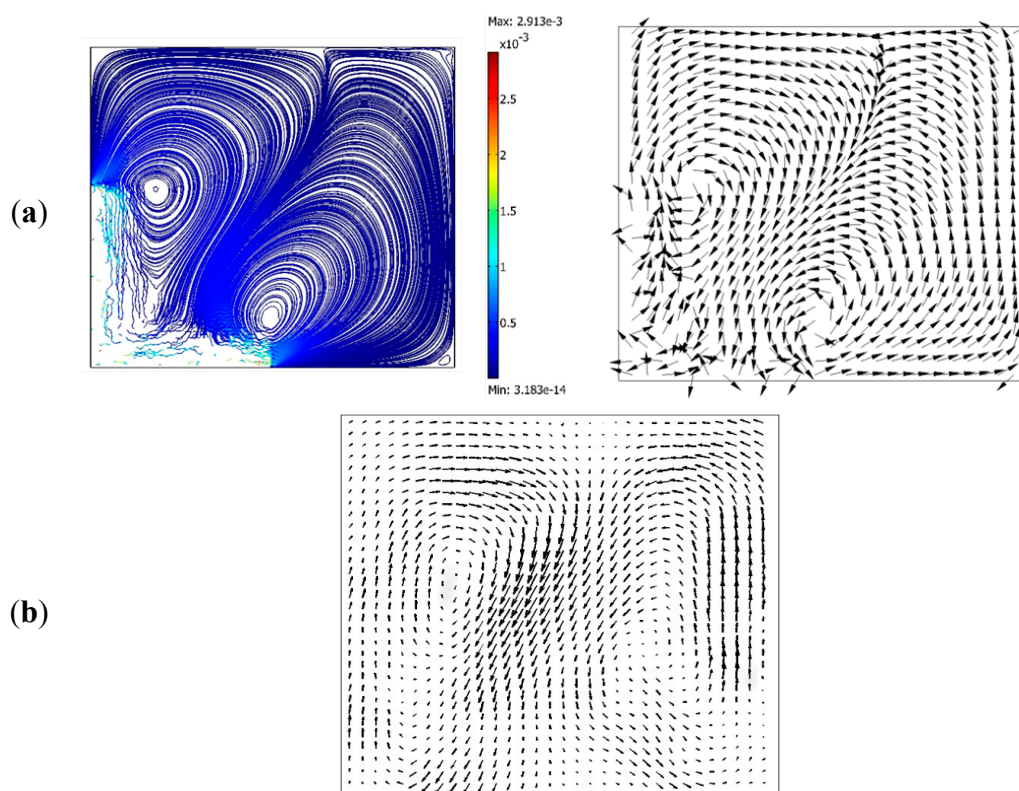

Figure 7 shows the formation of two large recirculation areas that cross the diagonal of the cuvette when the two transducers are simultaneously actuated. The attenuation and superposition of the acoustic pressure waves lead to a fluid movement pattern different from the one obtained when a single transducer is actuated, although the maximum velocities barely vary. Once again, the numerical and the experimental streaming results are in agreement.

When compared to a single transducer placed in the center of a cuvette face (top or bottom), as studied in previous works (as in reference [25] or [26]), the acoustic attenuation occurs from the centered acoustic source to the lateral and opposite walls, leading to the formation of two almost symmetric recirculation areas [25,26]. Previous works considered 110 μm PVDF films actuated at 10 MHz. However, by actuating the transducers at other frequencies (in MHz range), for the same

positioning geometries, the global flow profiles do not change, as verified through simulations in [25]. Therefore, it can be concluded that the position of the transducer relative to the fluidic domain has a great impact on the acoustic streaming flow.

3.2. Potential for Miniaturized Mixing

After simulation of the acoustic streaming numerical model at macro scale, by reducing the cuvette dimensions (Figure 1) to the micro scale, and solving the same model (described in Section 1.1), it is possible to assess the acoustic streaming potential for mixing in microfluidic devices. Therefore, the model was applied to a 0.8 mm width × 0.7 mm height cuvette. Two transducers arrangements were considered: one 0.4 mm length transducer as shown in Figure 1a); and two 0.4 mm length transducers in the same arrangement of Figure 1b), and the generated acoustic streaming flows are presented in Figure 8.

Figure 8. Velocity magnitude (m/s) with streamlines (**left**) and flow vectors (**right**), in the 0.8 mm width × 0.7 mm height microcuvette with 0.4 mm length transducers, after a stationary simulation of the second order Navier-Stokes equations, considering a 24 Vpp and 34.2 MHz oscillatory excitation. (**a**) One transducer. (**b**) Two perpendicular transducers.
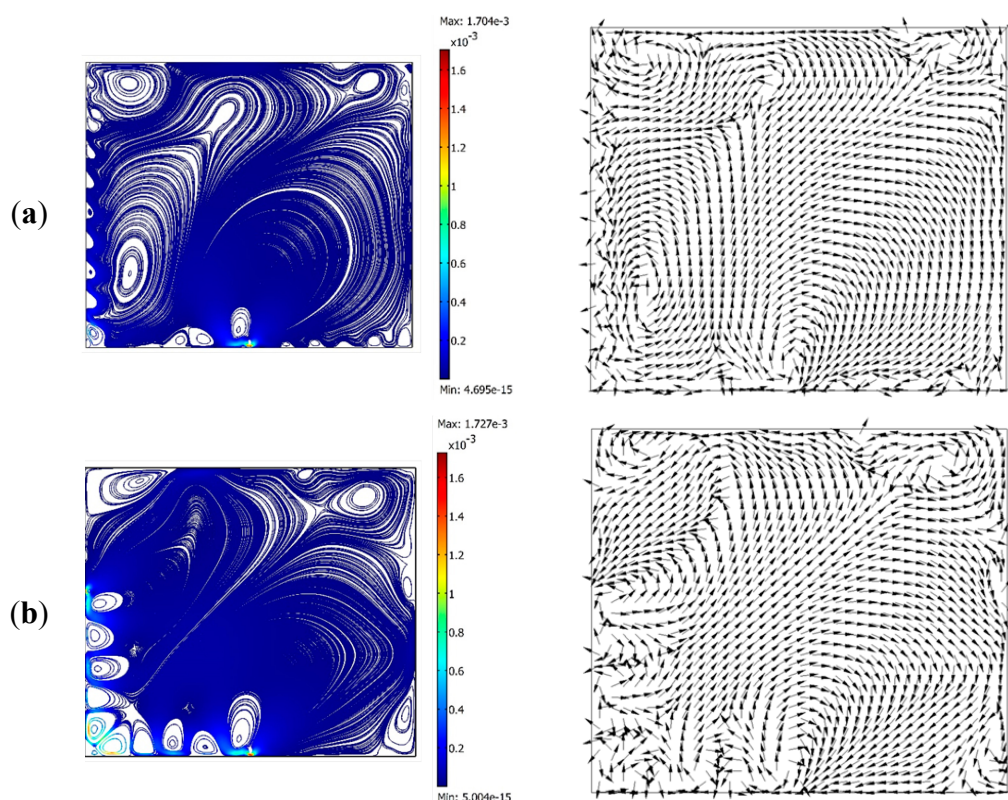
From Figure 8, the formation of two large recirculation areas is observed, as predicted for macro scale (Figures 6 and 7), where the streamlines are distributed over the whole domain. However, in microscale, the effect of the viscous boundary layer [27,32] is located near the transducer interfaces (lower left corner of Figure 8), where a lot of smaller recirculation areas are observed. This typical streaming flow is named Schlichting flow (more information about Schlichting flows can be found in [7]). The presence of the viscous boundary layer affects the acoustic streaming patterns and its thickness depends on the kinetic viscosity of the medium and on the wave angular frequency. The

boundary layer thickness is given by $\delta = \sqrt{2\nu/\omega}$, where δ is the viscous layer thickness, *v* the kinetic viscosity of the medium and ω the wave angular frequency [32]. As the microcuvette dimensions decrease, the viscous boundary layer effects become more relevant to the acoustic streaming flows.

The maximum streaming velocity achieved with two transducers (1.727 mm/s), obtained through numerical simulation, was slightly higher than the achieved with one transducer (1.704 mm/s). These results show that the actuation of β-PVDF piezoelectric transducers arranged in a perpendicular positioning may enhance the streaming. Moreover, due to its fabrication process, the β-PVDF has great potential for miniaturizing and integration in microfluidic devices. As the scale dimensions decrease, the mixing process becomes more difficult [27] and, therefore, simulation studies are essential to predict the fluids' behavior at microscale.

4. Conclusions

The paper reported a numerical and experimental study of the effect of β-PVDF piezoelectric transducers in the acoustic streaming patterns in a fluidic domain. Two transducer arrangements were studied: on one side, a 28 μm thick β-PVDF piezoelectric transducer was placed asymmetrically in the bottom left side of a cuvette containing the fluidic domain and, on the other side, two β-PVDF transducers were placed perpendicularly to each other, in the lower left corner of a cuvette. The results show that the number of transducers and their positioning affects the shape and the number of recirculation areas in the acoustic streaming flows and, therefore, affects the mixture.

When compared to the authors' previous works, where a single transducer was placed in the center of a cuvette face, the acoustic actuation lead to the formation of two large symmetric recirculation areas, which does not occur in the present work, showing that the position of the transducer relatively to the fluidic domain has a great impact on the acoustic streaming flow. Furthermore, when compared with the previous published works, this paper presents a comparison between numerical and experimental flows obtained by acoustic actuation of a β-PVDF transducer at 34.2 MHz.

These results show that the high frequency actuation of β-PVDF piezoelectric transducers, in addition to a great potential for miniaturizing and integration in microfluidic devices, can be an effective alternative for enhancing the streaming, due to the streaming patterns that cover the whole domain. The obtained global flows suggest that the presented transducer arrangements have great potential for mixing and pumping, being an alternative to the previous geometries studied by the authors.

Author Contributions

Susana O. Catarino and João Mário Miranda developed the mathematical model and performed the numerical simulations. The geometry design and experimental planning was performed by Susana O. Catarino and Graça Minas. All authors have analyzed the data. Susana O. Catarino has written the main manuscript and all authors reviewed the manuscript.

Conflicts of Interest

The authors declare no conflict of interest.

References

1. Suh, Y.K.; Kang, S. A review on mixing in microfluidics. *Micromachines* **2010**, *1*, 82–111.
2. Rife, J.C.; Bell, M.I.; Horwitz, J.S.; Kabler, M.N.; Auyeung, R.C.Y.; Kim, W.J. Miniature valveless ultrasonic pumps and mixers. *Sensors Actuators A Phys.* **2000**, *86*, 135–140.
3. Gantner, A.; Hoppe, R.H.W.; Köster, D.; Siebert, K.; Wixforth, A. Numerical simulation of piezoelectrically agitated surface acoustic waves on microfluidic biochips. *Comput. Vis. Sci.* **2006**, *10*, 145–161.
4. Frampton, K.D.; Minor, K.; Martin, S. Acoustic streaming in micro-scale cylindrical channels. *Appl. Acoust.* **2004**, *65*, 1121–1129.
5. Nguyen, N.-T.; White, R.M. Acoustic streaming in micromachined flexural plate wave devices: Numerical simulation and experimental verification. *IEEE Trans. Ultrason. Ferroelectr. Freq. Control* **2000**, *47*, 1463–1471.
6. Yeo, L.Y.; Friend, J.R. Surface acoustic wave microfluidics. *Annu. Rev. Fluid Mech.* **2014**, *46*, 379–406.
7. Wiklund, M.; Green, R.; Ohlin, M. Acoustofluidics 14: Applications of acoustic streaming in microfluidic devices. *Lab Chip* **2012**, *12*, 2438–2451.
8. Nguyen, N.-T.; Truong, T.-Q. A fully polymeric micropump with piezoelectric actuator. *Sensors Actuators B Chem.* **2004**, *97*, 137–143.
9. Köster, D. Numerical simulation of acoustic streaming on surface acoustic wave-driven biochips. *SIAM J. Sci. Comput.* **2007**, *29*, 2352–2380.
10. Rezk, A.R.; Qi, A.; Friend, J.R.; Li, W.H.; Yeo, L.Y. Uniform mixing in paper-based microfluidic systems using surface acoustic waves. *Lab Chip* **2012**, *12*, 773–779.
11. Riley, N. Acoustic streaming. *Theor. Comput. Fluid Dyn.* **1998**, *10*, 349–356.
12. Riley, N. Steady streaming. *Annu. Rev. Fluid Mech.* **2001**, *33*, 43–65.
13. Nyborg, W.L. Acoustic streaming due to attenuated plane waves. *J. Acoust. Soc. Am.* **1953**, *25*, 68.
14. Sencadas, V.; Gregorio Filho, R.; Lanceros-Mendez, S. Processing and characterization of a novel nonporous poly(vinilidene fluoride) films in the β phase. *J. Non. Cryst. Solids* **2006**, *352*, 2226–2229.
15. Sencadas, V.; Barbosa, R.; Mano, J.F.; Lanceros-Méndez, S. Mechanical characterization and influence of the high temperature shrinkage of β-PVDF films on its electromechanical properties. *Ferroelectrics* **2003**, *294*, 61–71.

16. Cardoso, V.F.; Catarino, S.O.; Serrado Nunes, J.; Rebouta, L.; Rocha, J.G.; Lanceros-Méndez, S.; Minas, G. Lab-on-a-chip with β-poly(vinylidene fluoride) based acoustic microagitation. *IEEE Trans. Biomed. Eng.* **2010**, *57*, 1184–1190.

17. Bar-Cohen, Y. *Electroactive Polymer (EAP) Actuators as Artificial Muscles: Reality, Potential and Challenges*, 2nd ed.; SPIE Press Book: Bellingham, WA, USA, 2004; pp. 89–139.

18. Ramadan, K.S.; Sameoto, D.; Evoy, S. A review of piezoelectric polymers as functional materials for electromechanical transducers. *Smart Mater. Struct.* **2014**, *23*, 033001.

19. Cardoso, V.F.; Minas, G.; Costa, C.M.; Tavares, C.J.; Lanceros-Mendez, S. Micro and nanofilms of poly(vinylidene fluoride) with controlled thickness, morphology and electroactive crystalline phase for sensor and actuator applications. *Smart Mater. Struct.* **2011**, *20*, 087002.

20. Eckart, C. Vortices and streams caused by sound waves. *Phys. Rev.* **1948**, *73*, 68–76.

21. Shilton, R.J.; Yeo, L.Y.; Friend, J.R. Quantification of surface acoustic wave induced chaotic mixing-flows in microfluidic wells. *Sensors Actuators B Chem.* **2011**, *160*, 1565–1572.

22. Luong, T.-D.; Phan, V.-N.; Nguyen, N.-T. High-throughput micromixers based on acoustic streaming induced by surface acoustic wave. *Microfluid. Nanofluid.* **2010**, *10*, 619–625.

23. Huang, X.Y.; Wen, C.-Y.; Jiao, Z.J. A standing wave model for acoustic pumping effect in microchannels. *Appl. Acoust.* **2010**, *71*, 164–168.

24. Ahmed, D.; Mao, X.; Shi, J.; Juluri, B.K.; Huang, T.J. A millisecond micromixer via single-bubble-based acoustic streaming. *Lab Chip* **2009**, *9*, 2738–2741.

25. Catarino, S.O.; Miranda, J.M.; Lanceros-Méndez, S.; Minas, G. Numerical prediction of acoustic streaming in a microcuvete. *Can. J. Chem. Eng.* **2014**, doi:10.1002/cjce.22057.

26. Catarino, S.O.; Miranda, J.M.; Lanceros-Mendez, S.; Minas, G. A numerical study on the heat transfer generated by a piezoelectric transducer in a microfluidic system. *J. Phys. Conf. Ser.* **2012**, *395*, 012091.

27. Frampton, K.D.; Martin, S.E.; Minor, K. The scaling of acoustic streaming for application in micro-fluidic devices. *Appl. Acoust.* **2003**, *64*, 681–692.

28. Nguyen, N.-T.; White, R.M. Design and optimization of an ultrasonic flexural plate wave micropump using numerical simulation. *Sensors Actuators A Phys.* **1999**, *77*, 229–236.

29. Pozar, D. *Microwave Engineering*, 3rd ed.; John Wiley & Sons: Hoboken, NJ, USA, 2005.

30. Thielicke, W.; Stamhuis, E.J. PIVlab—Time-Resolved Digital Particle Image Velocimetry Tool for MATLAB (version: 1.32). Available online: http://figshare.com/articles/PIVlab_version_1_35/1092508 (accessed on 27 August 2014).

31. Catarino, S.O.; Silva, L.R.; Mendes, P.M.; Miranda, J.M.; Lanceros-Mendez, S.; Minas, G. Piezoelectric actuators for acoustic mixing in microfluidic devices numerical prediction and experimental validation of heat and mass transport. *Sensors Actuators B Chem.* **2014**, doi:10.1016/j.snb.2014.08.030.

32. Loh, B.G.; Lee, D.R.; Kwon, K. Acoustic streaming pattern induced by longitudinal ultrasonic vibration in an open channel using particle imaging velocimetry. *Appl. Phys. Lett.* **2006**, *89*, 183505.